Hindawi
Journal of Chemistry
Volume 2021, Article ID 5556940, 13 pages
https://doi.org/10.1155/2021/5556940

Research Article

Removal of Methylene Blue from Aqueous Solutions by Using Nance (*Byrsonima crassifolia*) Seeds and Peels as Natural Biosorbents

Lorena Robles-Melchor,[1] **Maribel Cornejo-Mazón**,[1] **Diana Maylet Hernández-Martínez**,[1] **Gustavo F. Gutiérrez-López**,[2] **Santiago García-Pinilla**,[3] **Edgar Oliver López-Villegas**,[4] **and Darío Iker Téllez-Medina**[2]

[1]*Instituto Politécnico Nacional, Escuela Nacional de Ciencias Biológicas, Departamento de Biofísica, Carpio y Plan de Ayala S/N Santo Tomás 11340, Ciudad de México, Mexico*
[2]*Instituto Politécnico Nacional, Escuela Nacional de Ciencias Biológicas, Departamento de Ingeniería Bioquímica, Carpio y Plan de Ayala S/N Santo Tomás 11340, Ciudad de México, Mexico*
[3]*Facultad de Ingeniería de Alimentos, Fundación Universitaria Agraria de Colombia–Uniagraria, Calle 170 # 54a–10, C.P. 111166, Bogotá, Colombia*
[4]*Instituto Politécnico Nacional, Escuela Nacional de Ciencias Biológicas, Departamento de Investigación, Carpio y Plan de Ayala S/N 11340, Ciudad de México, Mexico*

Correspondence should be addressed to Maribel Cornejo-Mazón; maribelpabe2@hotmail.com

Received 6 January 2021; Accepted 23 March 2021; Published 16 April 2021

Academic Editor: Murat Senturk

Contamination of effluents with chemicals is a serious problem that impacts human health. Methylene blue is a cationic dye found frequently in industrial and urban sewages. In this work, dried grinded seeds and peels of nance were used as biosorbents in aqueous solutions at pH 7 and 10 (simulating urban and textile effluents) finding that Langmuir and Freundlich isotherms adequately described the sorption. Adsorption efficiencies were larger than 98% in all cases and slightly lower at pH 7 due to the closeness with the point of zero charge (pzc) of seeds and peels of nance (5.96 and 3.42, respectively). In all cases, Langmuir adsorption was favorable ($R_{La} < 1$), and Gibbs free energy of adsorption was negative indicating spontaneity, and since these values were larger than −80 but lower than 0 kJ/mol, the MB removal process was mainly due to physical interactions, a characteristic of physical adsorption. No significant differences were found amongst bulk mass transfer coefficients for the adsorption of both sorbents, indicating that both bioadsorbents had the same hydrodynamic and driving forces as well as depicted similar MB-adsorbent affinities. Interaction of MB with adsorbents was corroborated by FTIR spectroscopy, and the sorption was evidenced by scanning electron microscopy and image analysis which indicated that both adsorbents had fractal structures.

1. Introduction

Contamination of effluents greatly impacts ecosystems frequently causing eutrophication and adverse effects on human health including digestive, skin, cognitive, and vision. Methylthioninium chloride or methylene blue ($C_{16}H_{18}ClN_3S$) (MB) is a synthetic dye that has a thiazine structure, is a cationic compound also known as Swiss blue, and is a contaminant frequently found in urban and industrial discharges due to commercial activities [1]. MB is used in pharmaceutical, personal care, printing, leather, and textile industries and is frequently discharged to sewage from domestic households as well as from small- and medium-sized businesses. It is also employed in medicine to

treat methemoglobinemia [2] and exhibits antioxidant, antimalarial, antidepressant, and cardioprotective properties. On the contrary, MB has various harmful effects on human health such as headache, shortness of breath, and high blood pressure [3, 4].

Bioremediation of effluents has received a great deal of attention, and the removal of harmful contaminants as metal ions has been extensively studied by using bio-based adsorbents (mainly agricultural residues) as an alternative to the use of other chemical adsorbents. For instance, waste biomass of *Phaseolus vulgaris* has been used for the removal of lead (II) ions [5], and its husks were used as adsorbent for Cr (VI) removal [6, 7]. *Agave* biomass has been employed as a biosorbent for lead (Pb II) and copper (Cu II) from contaminated water [8]. Additionally, soybean and rice hulls were utilized for the adsorption of Hg from dilute aqueous solutions [9]. Also, the adsorption of Cd (II) was carried out by using citrus peels in a packed bed column [10], and the removal of basic fuchsin from water was carried out with mussel powdered eggshell membranes as the adsorbent [11].

The removal of MB by using biosorbents has also received attention. The adsorption of MB on *Citrus limetta* peel waste was studied with special focus on the associated costs and on the experimental fitting of data to various isotherm models [12]. Yan et al. [13] reported the sorption of methylene blue by using carboxymethyl cellulose, finding that the adsorption was dependent on pH, but independent of the temperature, and found that the Langmuir isotherm best fitted the experimental data. Aryee et al. [14] proposed the functionalization of peanut husk with iminodiacetic acid for the removal of MB from different solutions and reported mass transfer implications of the process. The adsorption of methylene blue on carbonaceous hydrochar derived from coffee husk waste as well as corresponding kinetics was also reported by Tran et al. [15]. Alver et al. [16] reported the adsorption of MB on alginate/rice husk biocomposite beads and found that pH did not influence sorption efficiency.

Nance fruit is consumed in tropical and subtropical countries and regions as in México and Central and South America, is a source of functional compounds [17, 18], and has been used at commercial levels to prepare soft drinks, ice cream, salads, and liquors [19]. Seeds and husks represent approximately 3 to 14% of the fresh fruit and are usually composted or disposed, and no other use has been given to these materials [19]. The seeds and peels of fruits of the family Malpighiaceae are rich in dietary fiber [20] which makes them potentially attractive biosorbents for cationic compounds such as methylene blue provided the charge balance on the adsorbents is negative [20]. Actually, there is one published report in which nance seeds were used as biosorbents for Cd (II) and Pb (II) in aqueous solutions, achieving percentages of removal up to 84% for Cd (II) to pH 8 and of 82% for Pb (II) to pH 5 [21]. Given the chemical characteristics of MB and nance seeds and peels, these materials are potential biosorbents for the removal of MB from aqueous solutions at different pH values. Also, the usage of these materials would aid in the revalorization of food processing byproducts. The aim of this work was to study the possible use of seeds and peels of nance as biosorbents for the removal of methylene blue from aqueous solutions and to infer on chemical interactions between the dye and the biosorbents by means of isotherms' modeling and spectroscopic and image analyses of the materials before and after MB adsorption.

2. Materials and Methods

2.1. Raw Materials. Fresh nance was acquired from the local market of Iguala, Guerrero, México. Fruits suitable for consumption were chosen according to the Mexican standard NOM-120-SSA1-1994. Even yellow color of the skin and a size ranging 1.5–2.0 cm in diameter were set as the criteria of commercial maturity [22]. Selected fruits were washed in running water, immersed in a 100 ppm sodium hypochlorite solution for 3 minutes, and rinsed with running water and finally with distilled water as reported by Díaz [22].

2.2. Separation of the Pulp and Collection of Husks and Seeds. Nance fruits were fed to a pulper machine (POLI, DERE-1, 022.301107.09, México) fitted with a 0.1 mm mesh to separate the pulp from seeds and peels which were collected and oven-dried (Thelco, Precision Scientific Company, model 19) until a $4 \pm 1\%$ moisture content (mc) wet basis was reached [23–25]. Dried samples were grinded by using a laboratory mortar and sieved to 60–200 mesh particles.

2.3. Proximal Analysis of Dried Seeds and Peels. Moisture content (AOAC 930.15), lipids (AOAC 983.23), crude fiber (AOAC 978.10), protein ($N \times 6.25$) (AOAC 955.04), ash (AOAC 923.03) and total carbohydrates (estimated by difference to 100%) were evaluated in the dried nance seeds and peels. All chemicals used were of analytical grade.

2.4. Point of Zero Charge (pzc). The point of zero charge was determined according to Albis et al. [20]. In brief, 50 mL of 0.01 M NaCl was adjusted to pH from 2 to 12 at 1 pH unit interval by using 0.01 M NaOH and HCl. Then, 0.1 g of the sorbents was added, and the mixture was stirred for 48 h. pH of each batch was measured (pH meter: Hach Sension 1, model 51700-23, China). Initial and final pH values were recorded and plotted. The pzc was found as pH of the intersection of plotted curves with a 45° straight line in the same graph [26].

2.5. Methylene Blue Adsorption Experiments. Adsorption experiments were carried out by preparing 10 MB solutions at different concentrations (25, 50, 75, 100, 125, 150, 175, 200, 225, and 250 ppm) [3, 8, 27]. Then, 0.1 g of the adsorbents (nance seeds and peels) was added, and pH was adjusted to 7 and 10 to simulate urban and industrial (textile) effluents [28]. Next, the systems were stirred for 4 h and filtered by using Whatman No. 40 filter paper. The filtrate was collected, and absorbance at 664 nm was measured and interpolated in a standard curve to finally determine the adsorbed mass of MB as follows:

$$q = \frac{(\mathrm{Co} - \mathrm{Ce})\, V}{m}, \tag{1}$$

in which q is the amount of adsorbed MB per unit mass of the adsorbent (mg/g), C_0 is the initial concentration of MB (mg/L), C_e is the final concentration of MB (mg/L), V is the volume of MB solution adsorbed (L), and m is the mass of the sorbent (g).

The percentage of MB removal or efficiency of adsorption (η) was obtained as follows:

$$\eta = \frac{\mathrm{Co} - \mathrm{Ce}}{\mathrm{Co}} \times 100. \tag{2}$$

Modelling of methylene blue adsorption is shown as follows.

Experimental adsorption data were fitted to Freundlich and Langmuir isotherms [29].

The Freundlich model is

$$q = K_F C_e^{\,1/n}, \tag{3}$$

in which q is the amount of adsorbed MB per unit mass of the adsorbent (mg/g), C_e is the concentration of MB at equilibrium (mg/g), K_F is Freundlich constant ((mg/g) $(\mathrm{L/mg})^{1/n}$), and n is Freundlich intensity constant (dimensionless).

In its logarithmic linear form, Freundlich isotherm is

$$\log q = \log K_F + \frac{1}{n} \log C_e. \tag{4}$$

By linear regression, the values of K_F and n can be obtained from the intercept and slope, respectively.

The Langmuir isotherm was applied to the sorption data as follows:

$$q = \frac{K_L C_e Q_{\max}}{1 + C_e K_L}. \tag{5}$$

In its linear form,

$$\frac{1}{q} = \frac{1}{Q_{\max}} + \frac{1}{K_L Q_m} \frac{1}{C_e}, \tag{6}$$

in which q is the amount of adsorbed MB per unit mass of the adsorbent (mg/g), K_L is Langmuir constant (L/mg), $Q_{\max}$ is the maximum adsorption (mg/g), and Ce is the residual concentration of the adsorbate (mg/L).

The Langmuir isotherm may be represented by the dimensionless equilibrium parameter (R_{La}) as given by Sayğılı et al. [29]:

$$R_{\mathrm{La}} = \frac{1}{1 + K_L C_0}, \tag{7}$$

in which K_L is Langmuir constant (L/mg) and C_0 is the initial concentration of methylene blue (mg/L). Values for R_{La} indicate various nature of isotherms such as irreversible ($R_{\mathrm{La}} = 0$), favorable ($0 < R_{\mathrm{La}} < 1$), linear ($R_{\mathrm{La}} = 1$), or unfavorable ($R_{\mathrm{La}} > 1$).

Efficiency of adsorption η was evaluated in all cases as [8]

$$\eta = \frac{C_0 - C_f}{C_i} \times 100, \tag{8}$$

in which C_i = and C_f are the initial and final concentrations of MB in the adsorbents.

2.6. Mass Transfer in Biosorption. The individual mass transfer coefficient for the liquid phase (k) at the onset of adsorption may be described by the rate equation [30]:

$$N = k_i\,(x_b - x_0), \tag{9}$$

in which N is the mass transfer flux (mg/h), k_i is the initial mass transfer coefficient (s^{-1}), x_b is the concentration of methylene blue in the bulk phase (liquid) at the beginning of the experiment, and x_0 is the concentration of methylene blue in the adsorbent (mg/g).

N can be obtained by dividing the amount of methylene blue adsorbed for each concentration of the colorant in the liquid by the four hours of duration of the adsorption, x_b can be considered as the initial concentration of the dye, and x_0 may, in every case, be considered as zero since at the beginning of the adsorption, the surface of the adsorbent is free of colorant.

2.7. Biosorption Thermodynamics. To investigate the change in Gibbs free energy, the following equation was applied [29]:

$$\Delta G^0 = -RT \ln K_L, \tag{10}$$

in which ΔG^0 is the change in Gibbs free energy (KJ/mol), R is the universal gas constant, T is the absolute temperature (K), and K_L is Langmuir constant (dimensionless).

2.8. Fourier-Transform Infrared Spectroscopy (FTIR). Nance seeds and peels were analyzed by FTIR [31] to detect functional groups before and after adsorption of MB. A Frontier FT-IR/NIR PerkinElmer Spectrometer, USA, fitted with a monolithic crystal was used. The spectral range varied from 4000 to 800 cm^{-1}.

2.9. Scanning Electron Microscopy and Image Analysis. Images of seeds and peels before and after methylene blue adsorption were obtained by scanning electron microscopy (SEM) (Quanta FEG 3D) (500x, 1500x, and 5000x, 15 kV, 26 pixels/nm^2) [32]. Fractal dimension (FD) was obtained by using ImageJ v. 1.53g software (National Institutes of Health, USA). Brightness and contrast for all images were adjusted automatically before performing the FracLac analysis. The size and greyscale values were standardized in all images using a calibrated greyscale. The fractal analysis was performed with the FracLac plugin in ImageJ software [33].

2.10. Statistical Analyses. Statistical analyses were carried out by means of an analysis of variance (ANOVA) by applying a significance level $\alpha = 0.05$. All calculations were carried out by using Minitab 17.1.0 software, and results were expressed as mean values ± standard deviation.

3. Results and Discussion

3.1. Proximal Analysis. The proximal analysis of nance seeds and peels is shown in Table 1. It was possible to observe that

Table 1: Proximal composition of nance peels and seeds (% wb)*.

	Method	Peels	Seeds
Moisture	AOAC 930.15	5.40 ± 0.30	5.30 ± 0.27
Lipids	AOAC 983.23	<0.10	<0.10
Crude fiber	AOAC 978.10	19.85 ± 0.99	19.94 ± 0.83
Protein (N × 6.25)	AOAC 955.04	4.30 ± 0.22	7.26 ± 0.36
Ash	AOAC 923.03	2.19 ± 0.12	2.08 ± 0.15
Total carbohydrates	Difference to 100%	68.26	65.42

*Mean values ± standard deviation.

both seeds and peels had substantial amounts of crude fiber which is their major component (19.85 and 19.94% for peels and seeds, respectively), making these materials attractive as potential biosorbents of a basic dye such as MB [29]. Even though there were no reports found on the composition of nance seeds and peels, it has been reported that the seeds of acerola cherry which belongs to the same family as nance (*Malpighia*) are a good source of dietary fiber [20].

3.2. Point of Zero Charge. The point of zero charge (pzc) of peels and seeds of nance was 3.42 and 5.96, respectively (Figure 1), and in this regard, Espinoza Rodríguez et al. [21] reported a pzc of 6.0 for nance seeds of an unknown variety. Obtained values of pzc indicated pH at which the materials had a zero net charge of the total particle surface as related to the media [34]. When sorption was carried out above pH values corresponding to the pzc, the negative sites on the surface of seeds and peels of nance will be exposed [35] and will present affinity by methylene blue if media pH is above the reported pKa for MB of 3.8 which favors the predominant cationic forms of this dye [36] that would be attracted to the negatively charged sites on the surface of the adsorbent in a way that efficient adsorption may be carried out at pH above 3.8. Thus, adsorption experiments were carried out at pH 7 and 10 for both bioadsorbents simulating urban and industrial (textile) effluents [28].

3.3. Sorption Isotherms. Methylene blue sorption isotherms are shown in Figures 2–5, and their corresponding constants are given in Table 2. It was possible to observe that Langmuir and Freundlich isotherm models fitted well ($R^2 > 0.99$ in all cases) to experimental data. Langmuir isotherm assumes ideal energetically homogeneous active sites and the consequent formation of a monolayer which leads to the assumption of a rather homogeneous structure of the adsorbent [29]. These considerations could well apply to MB adsorption onto cellulose and lignin which have polymeric structures [37], and the active sites are distributed rather evenly on the adsorbents, leading to rather homogeneous affinity for a comparatively small molecule as that of MB. Saygılı et al. [29] reported that Langmuir isotherm explained the adsorption of MB on dried grape pulp obtained after extraction of the juice. Similar values of K_L were obtained by Al-Anber et al. [38] when studying iron (III) adsorption on olive cake, by Alhujaily et al. [39] when removing anionic dyes from aqueous solutions using spent mushroom waste, and by Berber-Villamar et al. [40] who studied the adsorption of azo dye Direct Yellow 27 on corncob from aqueous solutions. It is noteworthy (Figures 2–5) that the slope of Freundlich and Langmuir isotherms corresponding to pH 10 was slightly larger than that at pH 7. This was due to the relatively higher affinity between adsorbent and MB at pH 10, discussed in Section 3.4. Yan et al. [13] reported that the sorption of methylene blue on carboxymethyl cellulose was dependent on media pH. Additionally, all obtained values of the equilibrium parameter (R_{La}) were lower than 1 (Table 2) which indicated the favorable nature of the Langmuir isotherm for the sorption process [29].

Freundlich isotherm is empirical and considers a nonuniform adsorption and a heterogeneous sorption heat distribution during adsorption [29]. The exponent n suggests the nature of the sorbent's surface. Values lower than 1 but larger than 0 indicated a less heterogeneous surface of nance seeds and peels at both pH values (7 and 10), being slightly more favorable at pH 10. This was expected given the higher-affinity adsorbents-MB at this larger pH value as shown in Figures 6 and 7 [41], given its remoteness to pKa as described in Section 3.2. Also, it is suggested that, at values of $1/n \ll 1$, the surface is energetically heterogeneous than for $1/n$ figures closer to 1. Therefore, as $1/n$ for both materials was, in average, 0.99 and 0.96 for seeds and peels, respectively (Table 2), the adsorption of MB onto seeds and peels of nance took place on rather energetically homogeneous surfaces [41], being slightly more heterogeneous for peels than for seeds. Physical roughness was also found to be slightly more pronounced (higher fractal dimension) for peels than for seeds (Section 3.8).

3.4. Efficiency of Adsorption. Efficiencies of adsorption for both biosorbents are presented in Figures 6 and 7. It was possible to observe that, at pH 7, adsorption reached maximum values of 99 and 98% at MB concentrations of 75 and100 mg/L for peels and seeds, respectively. For the region of low initial concentrations of MB (25–75 mg/L), low adsorption efficiencies were obtained (Figures 6 and 7) [20]. This was due to the small amounts of dye molecules present in the media associated with low activity coefficients in the diluted solutions, causing small amounts of MB deposits on the active sites of the adsorbent. At high initial concentrations of MB, the efficiency remained rather constant, and the small decrements observed for seeds at pH 10 could be due to

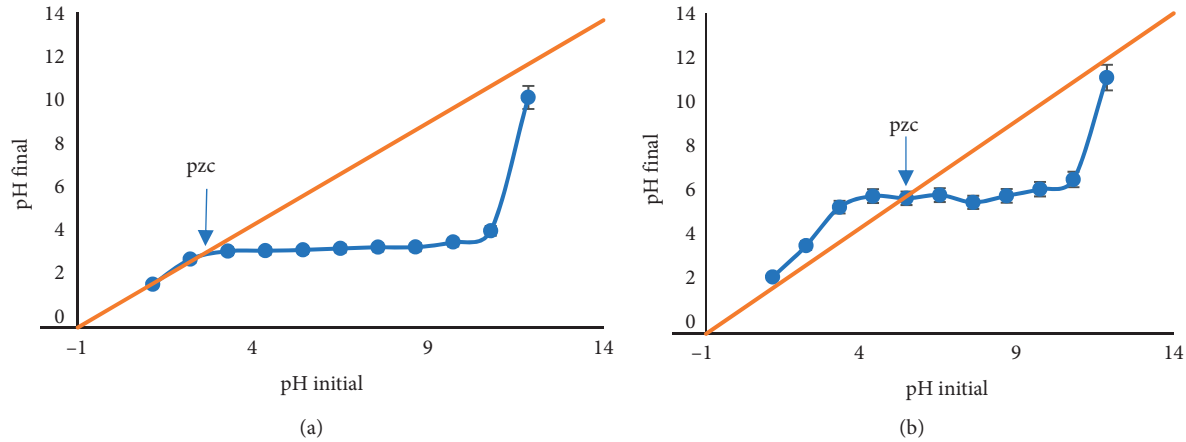

Figure 1: Point of zero charge (pzc) for peels (a) and seeds (b) of nance. pzc (pointed with the arrows) is found in the intersection of the 45° line with the experimental curve.

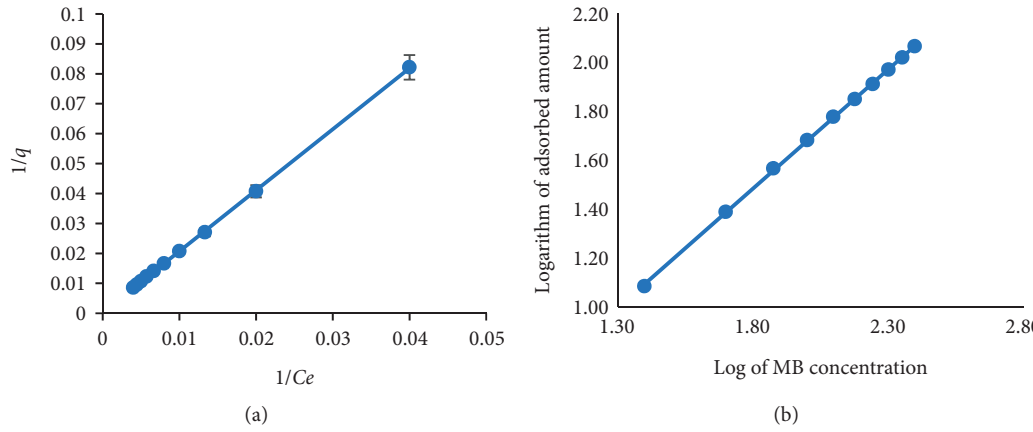

Figure 2: Sorption isotherms: Langmuir (a) and Freundlich (b) for nance peels at pH 7.

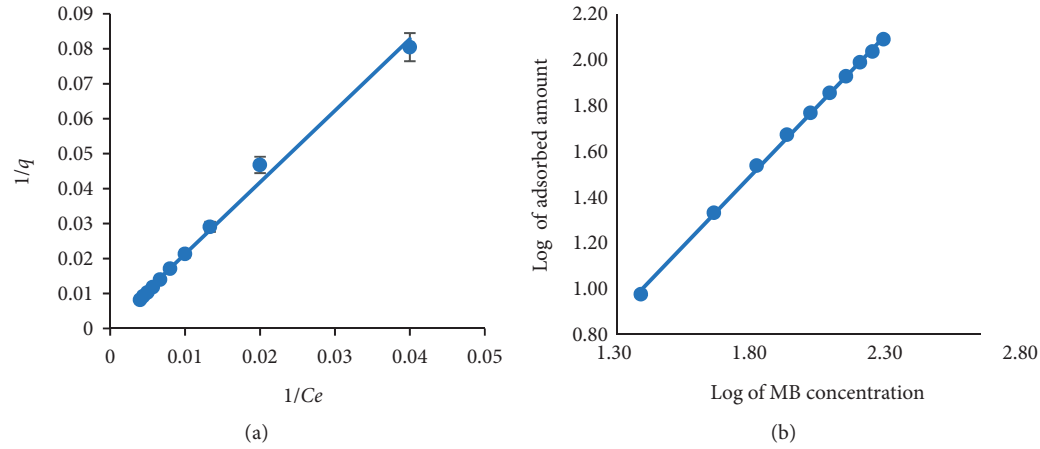

Figure 3: Sorption isotherms: Langmuir (a) and Freundlich (b) for nance peels at pH 10.

increased saturation of active sites for adsorption hence leaving residual MB in the media. Also, a higher pH value (10) caused MB to be positive charged, while cellulose and lignin of seeds and peels (Section 2.1) were predominantly negative [42] facilitating adsorption. Additionally, both polymers are reported to open their interlinked structures that form the fibers, exposing active sites and favoring adsorption at high pH [20].

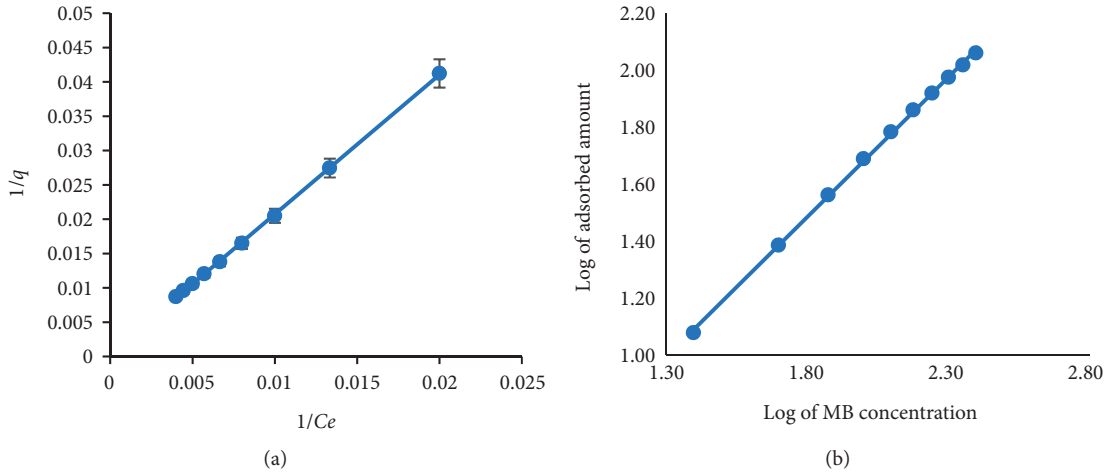

Figure 4: Sorption isotherms: Langmuir (a) and Freundlich (b) for nance seeds at pH 7.

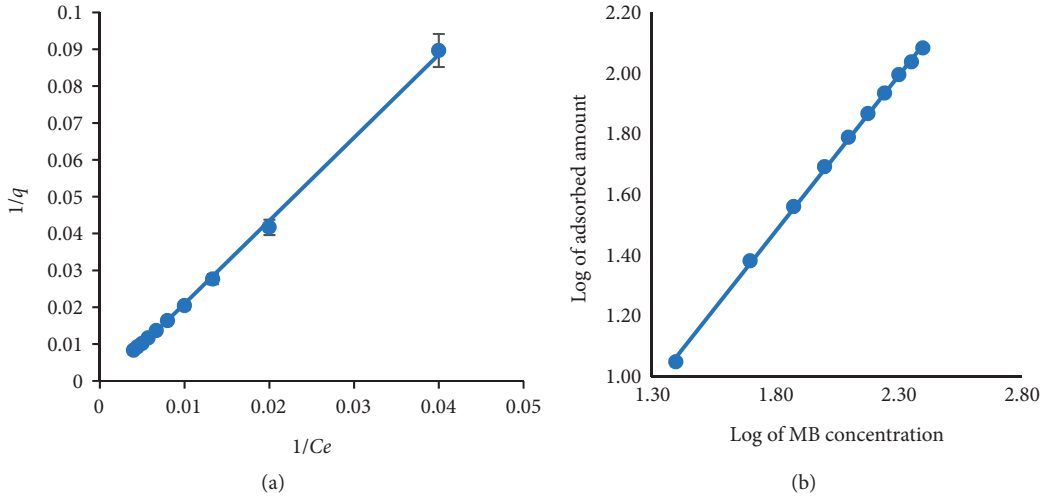

Figure 5: Sorption isotherms: Langmuir (a) and Freundlich (b) for nance seeds at pH 10.

Table 2: Constants for Langmuir and Freundlich isotherms corresponding to nance seeds and peels at pH 7 and 10.

Langmuir						Freundlich		
Biosorbent	Q_{max} (mg/g)	K_L (L/mg) $\times 10^{-3}$	R_{La}	R^2	ΔG^0 (kJ/mol)	K_F ((mg/g) (L/mg)$^{1/n}$)	n	R^2
Seeds (pH 7)	2553.80	1.92	0.95	0.9998	−1.5	0.52	1.017	0.9994
Seeds (pH 10)	7861.97	0.61	0.98	0.9998	−1.2	0.42	0.970	0.9994
Peels (pH 7)	2738.09	1.80	0.95	0.9999	−1.5	0.54	1.026	0.9997
Peels (pH 10)	1236.04	3.95	0.91	0.9929	−1.7	0.28	0.906	0.9990

Q_{max}: maximum capacity of adsorption (mg/g); K_L: affinity constant (L/mg); R^2: correlation coefficient; PRESS: predicted residual error sum of squares.

3.5. Biosorption Thermodynamics. Change in Gibbs free energy was evaluated according to equation (10). Results of ΔG^0 obtained for the two sorbents at the two experimental pH values (7 and 10) are shown in Table 2. All values of ΔG^0 were negative which indicated that the biosorption process was spontaneous within the experimental conditions used, and these values were larger than −80 but lower than 0 kJ/mol which indicated that the MB adsorption process was due to physical interactions which are a characteristic of physical adsorption [29]. Larger ΔG^0 figures are associated to covalent binding between the adsorbent matrix and the adsorbate and are typical of chemisorption [38].

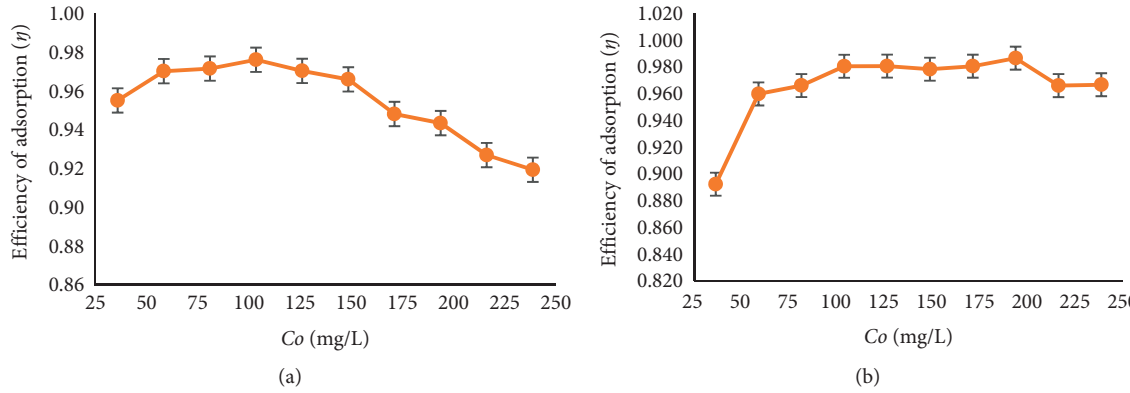

Figure 6: Nance seeds: effect of initial concentration (C_0) of MB on the efficiency of adsorption at pH 7 (a) and pH 10 (b).

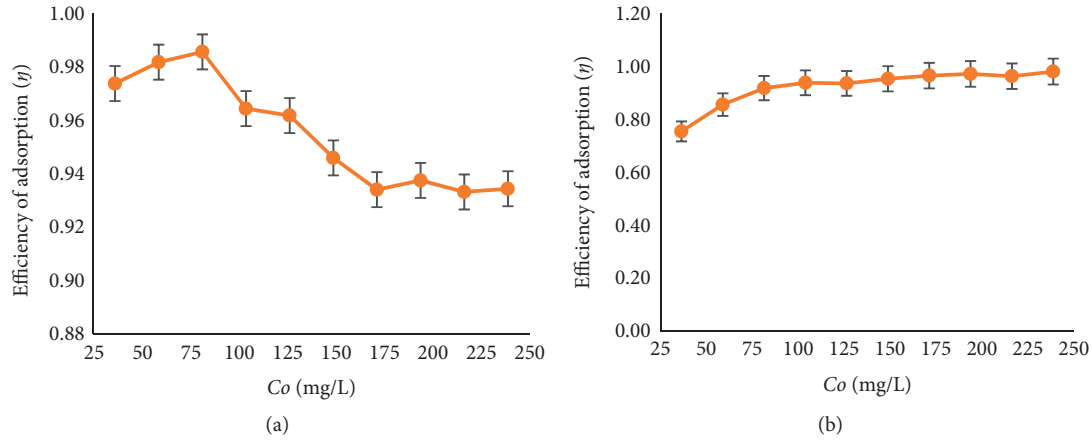

Figure 7: Nance peels: effect of initial concentration (C_0) of MB on the efficiency of adsorption at pH 7 (a) and pH 10 (b).

3.6. Bulk Mass Transfer Coefficients. Average bulk mass transfer coefficients corresponding to the onset of the adsorption are shown in Table 3. No significant differences were found amongst all mass transfer coefficients of both sorbents and pH values which indicated that both adsorbent systems had the same hydrodynamic and driving forces, as well as similar MB-adsorbent affinities at the beginning of the process, given that the surface of nance seeds and peels had irregular surfaces (Sections 3.3 and 3.8) and were free of dye at the onset of the adsorption. Obtained values of k were similar to those reported in [43] for the removal of phenol from wastewater using a forest waste. Knowledge of mass transfer coefficients and isotherms would greatly facilitate the design of an adsorbent system as well as the prediction of the optimum contact time between MB and the biosorbents [30]. Mass transfer to the solid includes transport of the solute from the bulk solution to the film around the adsorbent or film diffusion, internal diffusion from the film to the pores of the adsorbent, and adsorption on the external surface of the adsorbent on specific active sites [43]. Physical adsorption is practically instantaneous so that equilibrium is expected among the surface and the fluid at each location in the adsorbent particles [30].

Table 3: Average bulk mass transfer coefficients ($\times 10^{-5}$) for the onset of the adsorption ($s^{-1} \times 10^{-5}$)*.

	Seeds	Peels
pH 7	3.3 ± 0.3^a	3.3 ± 0.1^a
pH 10	3.2 ± 0.2^a	3.4 ± 0.4^a

Values ± standard deviation. *Different superscript letters in the same column indicate significant differences ($p \leq 0.05$).

3.7. FTIR Spectroscopy. In Figures 8–11, the FTIR spectra of bioadsorbents before and after MB removal are presented, and in Table 4, a summary of main bands detected as well as the type of bond interactions is shown. Both biosorbents presented bands as the O-H stretching at 3290 cm^{-1} corresponding to polysaccharides, lignin, and phenolic groups [44]; bands at 2924–2923 cm^{-1} and 2854 cm^{-1} which are characteristics of the C-H symmetric and nonsymmetric stretching, respectively, present in methyl and methylene groups of lipids, carotenoids, carboxylic groups, and lignin [45]. The decrement in peak intensities between 1370 and 1318 cm^{-1} corresponded to -OH, $-CH_2$, and $-CH_3$. Also, the C=O band at 1734 cm^{-1} gave place to two smaller peaks at 1743 and 1715 cm^{-1} that corresponded to interactions with

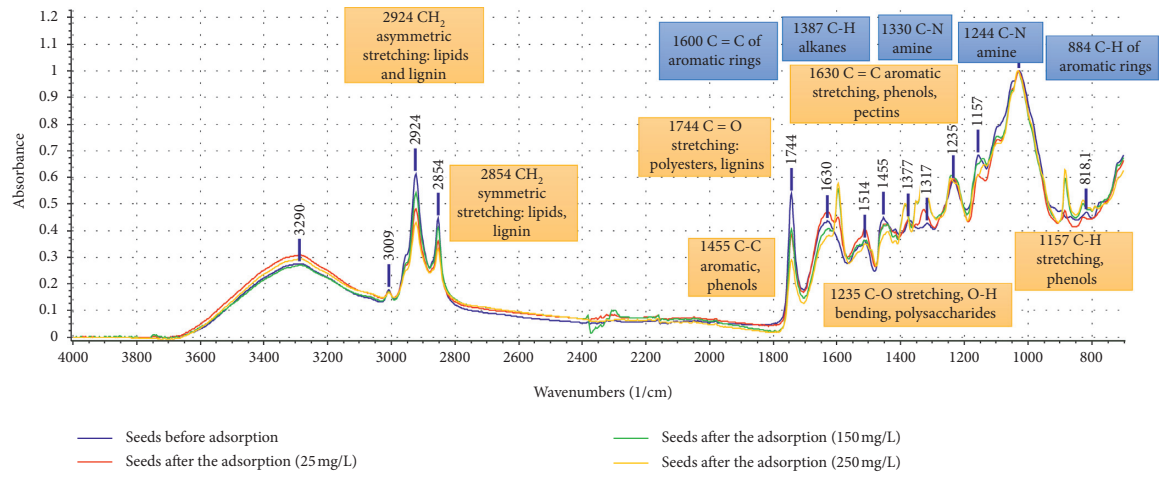

Figure 8: FTIR spectrum of nance seeds before and after MB adsorption (pH 7). Blue tags correspond to functional groups of MB. Orange tags correspond to functional groups of the seeds.

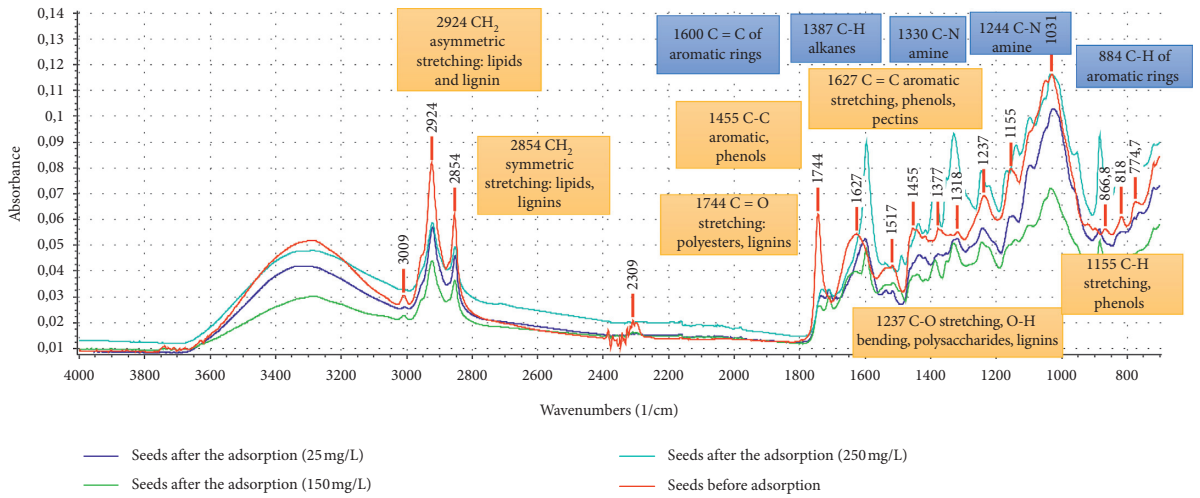

Figure 9: FTIR spectrum of nance seeds before and after MB adsorption (pH 10). Blue tags correspond to functional groups of MB. Orange tags correspond to functional groups of the seeds.

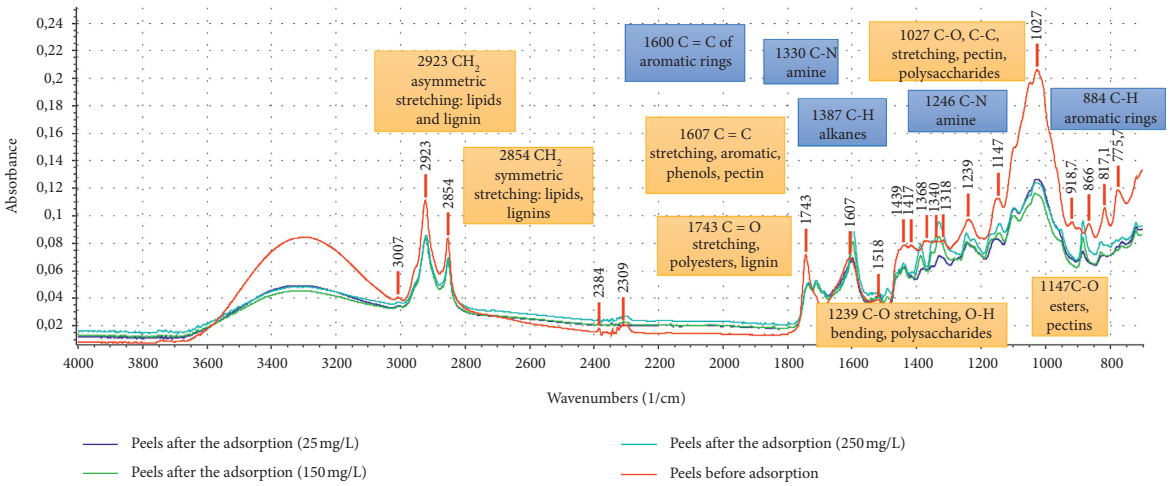

Figure 10: FTIR spectrum of nance peels before and after MB adsorption (pH 7). Blue tags correspond to functional groups of MB. Orange tags correspond to functional groups of the seeds.

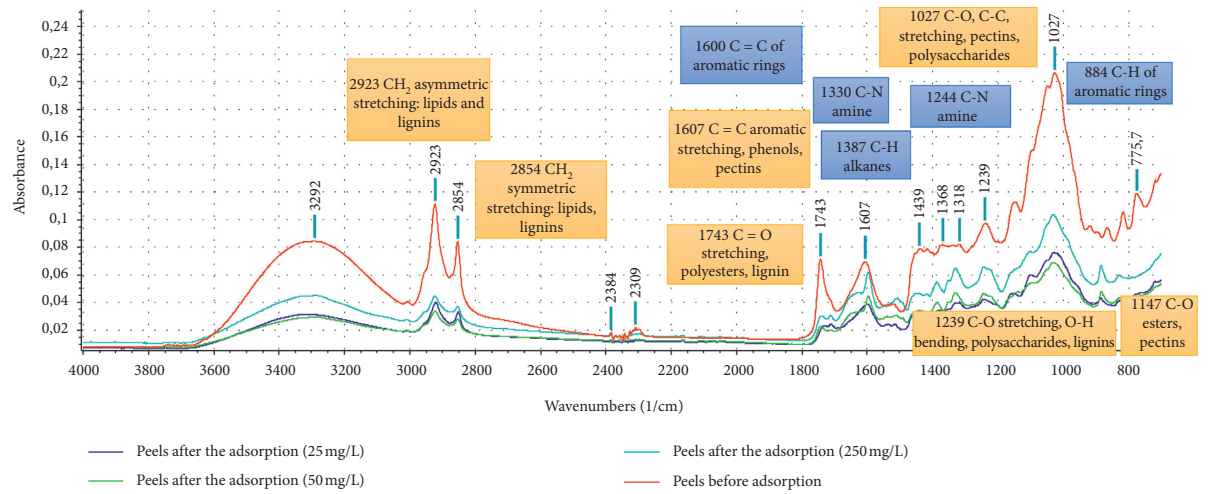

Figure 11: FTIR spectrum of nance peels before and after MB adsorption (pH 7). Blue tags correspond to functional groups of MB. Orange tags correspond to functional groups of the peels.

Table 4: Main functional groups and the FTIR spectra of nance seeds and peels.

Wavelength (cm^{-1})	Type of vibration	Compound	Nance seeds before adsorption	Nance seeds after adsorption (pH 7)	Nance seeds after adsorption (pH 10)	Nance peels before adsorption	Nance peels after adsorption (pH 7)	Nance peels after adsorption (pH 10)
3290	(O-H) ν	Polysaccharides, lignin, phenols	✓	✓	✓	✓	✓	✓
3007–3009	(=CH) ν	Lipids	✓	✓	✓	✓	✓	✓
2924–2923	(CH_2) ν, a (CH_3)ν, a	Lipids, lignin, carboxylic acids, carotenoids	✓	✓	✓	✓	✓	✓
2854	(CH_2) ν, s (CH_3)ν, a	Lipids, lignin, carboxylic acids, carotenoids	✓	✓	✓	✓	✓	✓
1743–1744	(C=O) ν	Polyesters, pectin, lignin, phenolic and carboxylic acids, lactones	✓	✓	✓	✓	✓	✓
1627–1630	(C=C) ν	Aromatic compounds, phenols, pectin, and carotenoids	✓	✓	✓			
1607	(C=C) ν	Aromatic compounds, phenols, and pectin.				✓	✓	✓
1600	(C=C) ν (C=N) ν	Methylene blue (aromatic rings)		✓	✓		✓	✓
1455	(C-C) δ	Aromatic compounds, phenols	✓	✓	✓			
1387	(C-H) δ	Methylene blue (alkane)		✓	✓		✓	✓
1370	(CH_2) δ, oop	Polysaccharides, pectin	✓	✓	✓	✓	✓	✓
1330–1331	(C-N) ν	Methylene blue (amine)		✓	✓		✓	✓
1318	(CH_2) δ, sc	Polysaccharides, pectin	✓	✓	✓	✓	✓	✓
1244–1246	(C-H) δ, oop	Methylene blue (amine)		✓	✓		✓	✓

Table 4: Continued.

Wavelength (cm^{-1})	Type of vibration	Compound	Nance seeds before adsorption	Nance seeds after adsorption (pH 7)	Nance seeds after adsorption (pH 10)	Nance peels before adsorption	Nance peels after adsorption (pH 7)	Nance peels after adsorption (pH 10)
1235–1239	(C-O) ν (O-H) δ	Polysaccharides, lignin, and pectin	✓	✓	✓	✓	✓	✓
1155–1157	(C-H) ν	Phenols	✓	✓	✓			
1147	(C-O) ν	Pectin				✓	✓	✓
1027–1031	(C-O) ν (C-C) ν	Polysaccharides, pectin, acids	✓	✓	✓	✓	✓	✓
884–890	(C-H) δ	Methylene blue (aromatic rings)		✓	✓		✓	✓
866	(C-H) δ	Aromatic compounds	✓	✓	✓	✓	✓	✓

ν: stretching; δ: bending; s: symmetric; a: asymmetric; oop: out of plane; sc: scissoring.

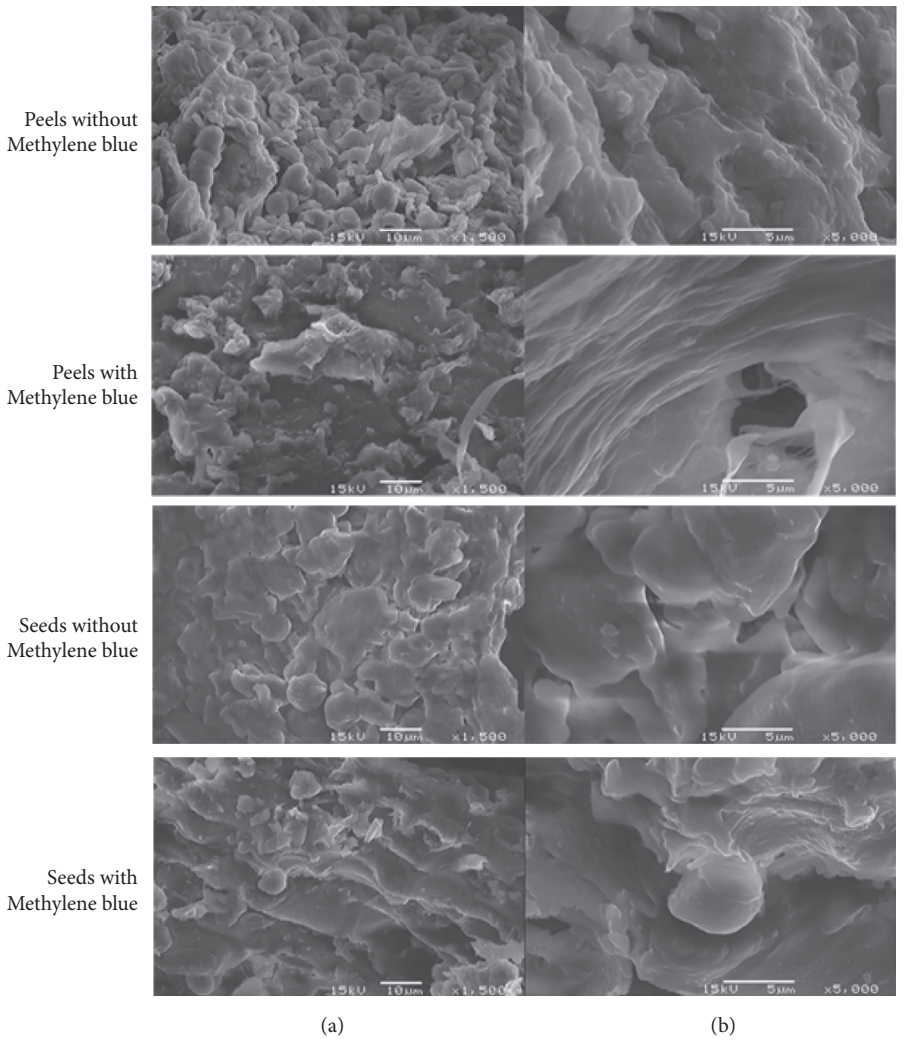

Figure 12: SEM images of the microstructure of adsorbents: peels (a) and seeds (b) before and after MB adsorption (1500x, 5000x, 15 kV).

MB [46]. Additionally, bands corresponding to C=C bonds of the aromatic rings and C=N of ammonia at 1600 cm^{-1}, C-H of methyl groups at 1387 cm^{-1}, C-N at 1330 cm^{-1}, C-H at 1244 cm^{-1}, and the bending of C-H of aromatic groups at 884 cm^{-1} [31, 45] which were not present in the spectra of the adsorbents without MB confirmed the presence of this dye after the adsorption. Overall, it was possible to observe that there were no major differences between adsorbents and

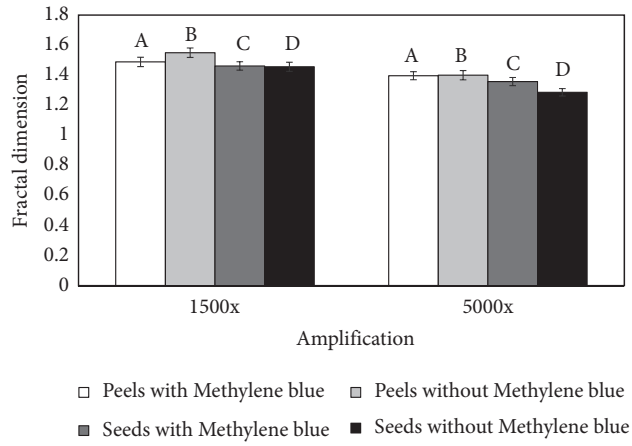

FIGURE 13: Fractal dimension of the SEM microstructure of adsorbents: peels and seeds before (B and D) and after (A and C) MB adsorption at 1500x and 5000x.

FTIR spectra at pH 7 and 10, and the presence of methylene blue after the adsorption was evident, confirming the suitability of nance seeds and peels to be used as biosorbents for the removal of MB from aqueous solutions.

3.8. Microstructure of Bioadsorbents and Image Analysis. SEM images (1500 and 5000x) of seeds and peels of nance before and after the MB adsorption are shown in Figure 12. Irregular surfaces were found in both biosorbents having fractal dimensions between 1.4 and 1.55 (Figure 13), and peels had a rougher structure (higher FD) than seeds. These findings agreed with values of constant n of the Freundlich isotherm as discussed in Section 3.3. In the case of peels at 1500x, it was possible to observe that the material without MB was more irregular (higher FD) ($p \leq 0.05$) than after the adsorption for which smoother structures could be observed which might be due to MB molecules covering the surface of the adsorbent [29], whereas seeds did not show significant differences ($p > 0.05$) before and after the adsorption. In the case of images at 5000x, seeds showed more homogeneous structures before than after the adsorption which might be due to scatter adsorption mechanisms during the formation of a monolayer.

4. Conclusions

Langmuir and Freundlich isotherms appropriately described the sorption of MB, and associated efficiencies were larger than 98% in all cases, being slightly lower for pH 7 due to the closeness with the point of zero charge (pzc) of seeds and peels of nance. At pH 7, adsorption reached maximum values of 99 and 98% at MB concentrations of 75 and 100 mg/L for peels and seeds, respectively. In all cases, Langmuir adsorption was favorable ($R_{La} < 1$) and spontaneous (negative Gibbs free energy of adsorption). The MB removal process was due to physical interactions, a characteristic of physical adsorption. No significant differences were found amongst bulk mass transfer coefficients for both adsorbents indicating that both adsorbent systems had similar hydrodynamic and driving forces under the conditions of the experiment. Adsorption of MB on the adsorbents was corroborated by FTIR spectroscopy and was mainly due to the presence of active sites distributed across complex polysaccharides in the biosorbents. The structure of adsorbents was evidenced by scanning electron microscopy and image analysis which indicated that both adsorbents had fractal and rougher structures, being more irregular in the peels than the seeds.

Data Availability

All the data used to support the findings of this study are available at Instituto Politécnico Nacional, Escuela Nacional de Ciencias Biológicas, Departamento de Biofísica, México.

Conflicts of Interest

The authors declare no conflicts of interest.

Acknowledgments

The authors are grateful to Instituto Politécnico Nacional (México) for the financial support to carry out this research under Grant nos. SIP 20181838, 20196469, and 20202010. This research was supported by Consejo Nacional de Ciencia y Tecnología (CONACYT), México, and Instituto Politécnico Nacional (IPN), México.

References

[1] K. Jalali, E. Pajootan, and H. Bahrami, "Elimination of hazardous methylene blue from contaminated solutions by electrochemically magnetized graphene oxide as a recyclable adsorbent," *Advanced Powder Technology*, vol. 30, no. 10, pp. 2352–2362, 2019.

[2] E. S. H. Kwok and D. Howes, "Use of methylene blue in sepsis: a systematic review," *Journal of Intensive Care Medicine*, vol. 21, no. 6, pp. 359–363, 2006.

[3] Y.-R. Zhang, S.-Q. Wang, S.-L. Shen, and B.-X. Zhao, "A novel water treatment magnetic nanomaterial for removal of anionic and cationic dyes under severe condition," *Chemical Engineering Journal*, vol. 233, pp. 258–264, 2013.

[4] E. Pajootan, M. Arami, and M. Rahimdokht, "Discoloration of wastewater in a continuous electro-Fenton process using modified graphite electrode with multi-walled carbon nanotubes/surfactant," *Separation and Purification Technology*, vol. 130, pp. 34–44, 2014.

[5] A. S. Özcan, S. Tunali, T. Akar, and A. Özcan, "Biosorption of lead (II) ions onto waste biomass of Phaseolus vulgaris L.: estimation of the equilibrium, kinetic and thermodynamic parameters," *Desalination*, vol. 244, no. 1–3, pp. 188–198, 2009.

[6] S. Srivastava, S. Bhushan Agrawal, M. K. De Mondal et al., "Characterization, Isotherm and kinetic study of Phaseolus vulgaris husk as an innovative adsorbent for Cr(VI) removal," *Environmental Engineering*, vol. 33, no. 1, pp. 567–575, 2016.

[7] S. Srivastava, S. B Agrawal, M. K. De Mondal et al., "Fixed bed column adsorption of Cr(VI) from aqueous solution using nanosorbents derived from magnetite impregnated Phaseolus vulgaris husk," *Environmental Progress and Sustainable Energy*, vol. 38, no. 1, pp. 568–576, 2019.

[8] M. T. Hernández-Botello, J. L. Barriada-Pereira, M. S. De Vicente et al., "Determination of biosorption mechanism in biomass of agave, using spectroscopic and microscopic techniques for the purification of contaminated water," *Revista Mexicana de Ingeniería Química*, vol. 19, no. 1, pp. 215–226, 2020.

[9] A. M. Rizzuti, F. L. Ellis, and L. W. Cosme, "Biosorption of mercury from dilute aqueous solutions using soybean hulls and rice hulls," *Waste and Biomass Valorization*, vol. 6, no. 4, pp. 561–568, 2015.

[10] A. Chatterjee and S. Schiewer, "Biosorption of cadmium (II) ions by citrus peels in a packed bed column: effect of process parameters and comparison of different breakthrough curve models," *CLEAN-Soil, Air, Water*, vol. 39, no. 9, pp. 874–881, 2011.

[11] W. Bessashia, Y. Berredjem, Z. Hattab, and M. Bououdina, "Removal of Basic Fuchsin from water by using mussel powdered eggshell membrane as novel bioadsorbent: equilibrium, kinetics, and thermodynamic studies," *Environmental Research*, vol. 186, p. 109484, 2020.

[12] S. Shakoor and A. Nasar, "Removal of methylene blue dye from artificially contaminated water using citrus limetta peel waste as a very low cost adsorbent," *Journal of the Taiwan Institute of Chemical Engineers*, vol. 66, pp. 154–163, 2016.

[13] H. Yan, W. Zhang, X. Kan et al., "Sorption of methylene blue by carboxymethyl cellulose and reuse process in a secondary sorption," *Colloids and Surfaces A: Physicochemical and Engineering Aspects*, vol. 380, no. 1–3, pp. 143–151, 2011.

[14] A. A. Aryee, F. M. Mpatani, A. N. Kani et al., "Iminodiacetic acid functionalized magnetic peanut husk for the removal of methylene blue from solution: characterization and equilibrium studies," *Environmental Science and Pollution Research*, vol. 27, no. 32, pp. 40316–40330, 2020.

[15] T. H. Tran, A. H. Le, T. H. Pham et al., "Adsorption isotherms and kinetic modeling of methylene blue dye onto a carbonaceous hydrochar adsorbent derived from coffee husk waste," *Science of the Total Environment*, vol. 725, p. 138325, 2020.

[16] E. Alver, A. Ü. Metin, and F. Brouers, "Methylene blue adsorption on magnetic alginate/rice husk bio-composite," *International Journal of Biological Macromolecules*, vol. 154, pp. 104–113, 2020.

[17] E. Martínez-Moreno, T. Corona-Torres, T. Corona-Torres et al., "Caracterización morfométrica de frutos y semillas de nanche (Byrsonima crassifolia (L.) H.B.K.)," *Revista Chapingo Serie Horticultura*, vol. 12, no. 1, pp. 11–17, 2006.

[18] S. F. Rivas-Castro, E. Martínez-Moreno, I. Alia-Tejacal, and A. Pérez-López, "Physical and physiological changes in phenotypes of nance [Byrsonima crassifolia (L.) H.B.K.] with different harvest maturity," *Scientia Horticulturae*, vol. 256, p. 108620, 2019.

[19] R. Medina-Torres, S. Salazar-Garcĺa, and J. R. Gómez-Aguilar, "Fruit quality indices in eight nance [byrsonima crassifolia (L.) H.B.K.] selections," *HortScience*, vol. 39, no. 5, pp. 1070–1073, 2004.

[20] A. Albis, H. Llanos, J. Galeano, and D. García, "Adsorción de azul de metileno utilizando cáscara de yuca (Manihot esculenta) modificada químicamente con ácido oxálico," *Revista Ion*, vol. 31, no. 2, pp. 99–110, 2018.

[21] M. Á. Espinosa Rodríguez, R. Delgado Delgado, A. Hidalgo Millán, L. Olvera Izaguirre, and L. A. Bernal Jácome, "Adsorción de Cd (II) y Pb (II) presentes en solución acuosa con hueso de nanche (Byrsonima crassifolia)," *Revista Colombiana de Química*, vol. 49, no. 2, pp. 30–36, 2020.

[22] F. López-Gálvez,, A. Allende, P. Truchado et al., "Suitability of aqueous chlorine dioxide versus sodium hypochlorite as an effective sanitizer for preserving quality of fresh-cut lettuce while avoiding by-product formation," *Postharvest Biology and Technology*, vol. 55, pp. 53–60, 2002.

[23] S. B. D. Alami, "Aprovechamiento de hueso de aceituna: biosorción de iones métalicos," Doctoral dissertation, Universidad De Granada, Granada, Spain, 2010.

[24] P. E. Ríos Elizalde, "Cinética de bioadsorción de arsénico utilizando cáscara de banano maduro en polvo," Bachelor's thesis, Universidad Técnica de Machala, Machala, Ecuador, 2014.

[25] J. C. Muñoz Carpio and N. J. Tapia Huanambal, *Biosorción De Plomo (II) Por Cáscara De naranja "Citrus Cinensis" Pretratada (Tesis De Pregrado Inédita)*, Universidad Nacional Mayor de San Marcos, Lima, Perú, 2007.

[26] A. A. Izuagie, W. M. Gitari, and J. R. Gumbo, "Synthesis and performance evaluation of Al/Fe oxide coated diatomaceous earth in groundwater defluoridation: towards fluorosis mitigation," *Journal of Environmental Science and Health, Part A*, vol. 51, no. 10, pp. 810–824, 2016.

[27] M. A. K. M. Hanafiah, W. S. W. Ngah, S. H. Zolkafly, L. C. Teong, and Z. A. A. Majid, "Acid Blue 25 adsorption on base treated Shorea dasyphylla sawdust: kinetic, isotherm, thermodynamic and spectroscopic analysis," *Journal of Environmental Sciences*, vol. 24, no. 2, pp. 261–268, 2012.

[28] R. Roy, A. N. M. Fakhruddin, R. Khatun, and M. S. Islam, "Reduction of COD and pH of textile industrial effluents by aquatic macrophytes and algae," *Journal of Bangladesh Academy of Sciences*, vol. 34, no. 1, pp. 9–14, 2010.

[29] H. Sayğılı, G. Akkaya Sayğılı, and F. Güzel, "Using grape pulp as a new alternative biosorbent for removal of a model basic dye," *Asia-Pacific Journal of Chemical Engineering*, vol. 9, no. 2, pp. 214–225, 2014.

[30] M. Mutlu and V. Gökmen, "Determination of effective mass transfer coefficient (Kc) of patulin adsorption on activated carbon packed bed columns with recycling," *Journal of Food Engineering*, vol. 35, no. 3, pp. 259–266, 1998.

[31] O. V. Ovchinnikov, A. V. Evtukhova, T. S. Kondratenko, M. S. Smirnov, V. Y. Khokhlov, and O. V. Erina, "Manifestation of intermolecular interactions in FTIR spectra of methylene blue molecules," *Vibrational Spectroscopy*, vol. 86, pp. 181–189, 2016.

[32] V. Freyre-Fonseca, D. I. Téllez-Medina, E. I. Medina-Reyes et al., "Morphological and physicochemical characterization of agglomerates of titanium dioxide nanoparticles in cell culture media," *Journal of Nanomaterials*, vol. 2016, 2016.

[33] S. García-Pinilla, G. F. Gutiérrez-López, H. Hernández-Sánchez, G. Cáez-Ramírez, E. García-Armenta, and L. Alamilla-Beltrán, "Quality parameters and morphometric characterization of hot-air popcorn as related to moisture content," *Drying Technology*, vol. 39, pp. 1–13, 2019.

[34] G. V. Franks and L. Meagher, "The isoelectric points of sapphire crystals and alpha-alumina powder," *Colloids and Surfaces A: Physicochemical and Engineering Aspects*, vol. 214, no. 1–3, pp. 99–110, 2003.

[35] F. A. A. Villa and A. H. Anaguano, "Determination of the point of zero charge and isoelectric point of two agricultural wastes and their application in the removal of colorants," *Revista de Investigación Agraria y Ambiental*, vol. 4, no. 2, pp. 27–37, 2013.

[36] D. Kong and L. D. Wilson, "Uptake of methylene blue from aqueous solution by pectin-chitosan binary composites," *Journal of Composites Science*, vol. 4, no. 3, p. 95, 2020.

[37] S. Morales-delaRosa and J. M. Campos-Martin, "Catalytic processes and catalyst development in biorefining," in *Advances in Biorefineries*, pp. 152–198, Woodhead Publishing, Cambridge, UK, 2014.

[38] Z. A. Al-Anber and M. A. Al-Anber, "Thermodynamics and kinetic studies of iron (III) adsorption by olive cake in a batch system," *Journal of the Mexican Chemical Society*, vol. 52, no. 2, pp. 108–115, 2008.

[39] A. Alhujaily, H. Yu, X. Zhang, and F. Ma, "Adsorptive removal of anionic dyes from aqueous solutions using spent mushroom waste," *Applied Water Science*, vol. 10, no. 7, pp. 1–12, 2020.

[40] N. K. Berber-Villamar, A. R. Netzahuatl-Muñoz, L. Morales-Barrera, GM. Cha´vez-Camarillo, and C. M. Flores-Ortiz, "Cristiani-Urbina E Corncob as an effective, eco-friendly, and economic biosorbent for removing the azo dye direct yellow 27 from aqueous solutions," *PLoS One*, vol. 13, no. 4, Article ID e0196428, 2018.

[41] M. A. Al-Ghouti and D. A. Da'ana, "Guidelines for the use and interpretation of adsorption isotherm models: a review," *Journal of Hazardous Materials*, vol. 393, p. 122383, 2020.

[42] E. C. Medina, A. M. G. Hinojos, and A. V. Rodríguez, "Estudio de la remoción del colorante azul de metileno empleando la biomasa de la morinda citrocifolia L. *Quivera*," *Revista de Estudios Territoriales*, vol. 13, no. 2, pp. 52–62, 2011.

[43] C. R. Girish and V. R. Murty, "Mass transfer studies on adsorption of phenol from wastewater using Lantana camara, forest waste," *International Journal of Chemical Engineering*, vol. 2016, 2016.

[44] J. Nogales-Bueno, B. Baca-Bocanegra, A. Rooney, J. M. Hernández-Hierro, H. J. Byrne, and F. J. Heredia, "Study of phenolic extractability in grape seeds by means of ATR-FTIR and Raman spectroscopy," *Food Chemistry*, vol. 232, pp. 602–609, 2017.

[45] G. Socrates, *Infrared and Raman Characteristic Group Frequencies: Tables and Charts*, John Wiley & Sons, Hoboken, NJ, USA, 2004.

[46] A. Gürses, A. Hassani, M. Kıranşan, Ö. Açışlı, and S. Karaca, "Removal of methylene blue from aqueous solution using by untreated lignite as potential low-cost adsorbent: kinetic, thermodynamic and equilibrium approach," *Journal of Water Process Engineering*, vol. 2, pp. 10–21, 2014.